AIP | Review of Scientific Instruments

Mass determination and sensitivity based on resonance frequency changes of the higher flexural modes of cantilever sensors

John D. Parkin and Georg Hähner

Citation: Review of Scientific Instruments **82**, 035108 (2011); doi: 10.1063/1.3563724

View online: http://dx.doi.org/10.1063/1.3563724

View Table of Contents: http://scitation.aip.org/content/aip/journal/rsi/82/3?ver=pdfcov

Published by the AIP Publishing

Mass determination and sensitivity based on resonance frequency changes of the higher flexural modes of cantilever sensors

John D. Parkin and Georg Hähner[a)]
EaStCHEM School of Chemistry, University of St. Andrews, North Haugh, St. Andrews, KY16 9ST, United Kingdom

(Received 7 January 2011; accepted 16 February 2011; published online 10 March 2011)

Micro- and nanocantilevers are increasingly employed as mass sensors. Most studies consider the first flexural mode and adsorbed masses that are either discretely attached or homogeneously distributed along the entire length of the cantilever. We derive general expressions that allow for the determination of the total attached mass with any mass distribution along the cantilever length and all flexural modes. The expressions are valid for all cantilevers whose flexural deflection can be described by a one-dimensional function. This approach includes the most common types of microcantilevers, namely, rectangular, picket, and V-shaped. The theoretical results are compared with experimental data up to the fourth flexural mode obtained from thermal noise spectra of rectangular and V-shaped cantilevers. © *2011 American Institute of Physics*. [doi:10.1063/1.3563724]

I. INTRODUCTION

Micro- and nanocantilever sensors are attracting an increasing amount of attention due to their wide availability and outstanding sensing capabilities, e.g., see Refs. 1–4. One area that is currently of significant interest is mass sensing,[5] where one of the goals is to achieve highest mass sensitivity with micro- and nanomechanical devices.[6] It has been demonstrated that such devices are capable of detecting single cells,[7] bacteria,[8] and even single biological molecules.[9] In the context of mass sensing determination of masses that are nonhomogenously distributed or that are only attached in specific areas along the cantilever is of pivotal importance since cantilevers can be modified accordingly.[4] Mass sensing based on the frequency changes of the flexural modes that are due to one or two discretely attached masses[10,11] as well as a homogeneous mass distribution along the full length of the cantilever in connection with the first flexural mode have been reported in the literature, e.g., see Ref. 12. However, there is no general description relating the frequency changes of the higher flexural modes to an attached mass that is homogeneously or nonhomogeneously distributed along the cantilever. Even the discrete attachment of small spheres to microcantilevers[10,11] does, strictly speaking, create a mass distribution localized around the positions of the spheres. The size and weight of the attached masses determine whether a point mass model is still valid. In case of single objects which cannot be described by a point mass[13] or if the mass is distributed over a certain region of the plan view area of the cantilever, a proper mass model has to be used to describe the oscillation behavior and the resulting frequency change of the cantilever correctly. Knowledge of the effective oscillating cantilever mass related to the flexural modes is therefore crucial for a quantification of the adsorbed mass. In the following we derive general expressions for the effective oscillating cantilever mass and of the frequency shifts that are caused by an arbitrary distribution of a mass attached along a cantilever for all flexural modes. The cantilever can be of any shape as long as its true flexural deflection can be approximated by a function that only depends on the coordinate along the cantilever length. This is the case for the most common types of microcantilevers, namely, rectangular, picket, and V-shaped.[14] The results are expressed in terms of the modal shapes of the free cantilevers and their oscillating frequencies. The formulas allow for the determination of the total attached mass under any mass distribution. To test the theoretical findings we compare them with experimental data obtained from thermal noise spectra of rectangular and V-shaped cantilevers.

II. THEORETICAL BACKGROUND

If a small external mass is attached to a cantilever its dynamic properties will change according to the additional effective mass. In the following we assume that the total external mass is small compared to the total mass of the cantilever and that the external mass per unit area is constant over the dimension of the cantilever width. The external mass per unit length $\Delta m_{\mathrm{ext}}(x)$ is determined by the density of the external mass, $\rho_{m,\mathrm{ext}}(x)$, the width of the beam, $w(x)$, and the thickness of the layer, $t_{\mathrm{ext}}(x)$: $\Delta m_{\mathrm{ext}}(x) = \rho_{m,\mathrm{ext}}(x) S_{m,\mathrm{ext}}(x)$, with $S_{m,\mathrm{ext}}(x) = w(x) t_{\mathrm{ext}}(x)$. This equation can be rewritten as $\Delta m_{\mathrm{ext}}(x) = \Delta \hat{m}_{\mathrm{ext}} \varphi(x) w(x)$, where $\Delta \hat{m}_{\mathrm{ext}}$ is the maximum value of the mass per unit area and $\varphi(x)$ describes the variation of the mass along the cantilever length. The total external mass acting on the cantilever is $\Delta M_{\mathrm{ext}} = \int_0^L \Delta m_{\mathrm{ext}}(x) dx$, where L is the cantilever length. The external mass causes a shift $\Delta(\omega_n^2) = \omega_n^2 - \hat{\omega}_n^2$ in the eigenfrequency of the nth flexural mode, with $\hat{\omega}_n$ being the resonant frequency with external mass and ω_n being the unperturbed resonant frequency without additional mass. The relation between the unperturbed resonant frequency, ω_n, the total external mass, ΔM_{ext}, and

[a)]Electronic mail: gh23@st-andrews.ac.uk. Fax: +44 1334 463808. Telephone: +44 1334 463889.

the resulting shift in the resonant frequency of the nth mode, $\Delta(\omega_n{}^2)$, of the cantilever is

$$\Delta(\omega_n^2) = -\omega_n^2 \frac{\Delta M_{\text{ext}}}{M_{\text{eff},n}^{\text{cant}}}, \tag{1}$$

where $M_{\text{eff},n}^{\text{cant}}$ is the effective oscillating mass of the cantilever in the nth mode. If the total external mass is small compared to the cantilever mass such that it does not change the shape of the eigenmodes, $u_n(x)$, of the cantilever significantly, then the total energy of the cantilever beam before and after adsorption is

$$\frac{1}{2}\omega_n^2 \int_0^L \rho(x)S(x)u_n^2(x)dx \approx \frac{1}{2}\hat{\omega}_n^2 \int_0^L \rho(x)S(x)u_n^2(x)dx + \frac{1}{2}\hat{\omega}_n^2 \int_0^L \rho_{\text{ext}}S_{\text{ext}}(x)u_n^2(x)dx, \tag{2}$$

where ρ and S refer to the density and the cross section of the cantilever, respectively. The eigenfunctions $u_n(x)$ can be normalized such that $\int_0^L \rho(x)S(x)u_n(x)u_m(x)dx = \delta_{nm}$.[15] Because of the normalization the relative frequency shifts $\Delta(\omega_n^2)/\omega_n^2$ are

$$\frac{\Delta(\omega_n^2)}{\omega_n^2} = -\int_0^L \rho_{\text{ext}}S_{\text{ext}}(x)u_n^2(x)dx = -\Delta\hat{m}_{\text{ext}} \int_0^L \varphi(x)w(x)u_n^2(x)dx. \tag{3}$$

Of practical interest is the total external mass, $\Delta M_{\text{ext}} = \Delta\hat{m}_{\text{ext}} \int_0^L \varphi(x)w(x)dx$, which can be obtained in combination with Eq. (3)

$$\Delta M_{\text{ext}} = -\frac{\Delta(\omega_n^2)}{\omega_n^2} \frac{\int_0^L \varphi(x)w(x)dx}{\int_0^L \varphi(x)w(x)u_n^2(x)dx}. \tag{4}$$

The effective mass of the cantilever, $M_{\text{eff},n}$, in the nth flexural mode is therefore

$$M_{\text{eff},n}^{\text{cant}} = \frac{\int_0^L \varphi(x)w(x)dx}{\int_0^L \varphi(x)w(x)u_n^2(x)dx}. \tag{5}$$

Note that the effective mass of the cantilever can be lower as well as higher than the actual mass of the cantilever $M = \int_0^L \rho(x)S(x)dx$, depending on the external mass distribution $\varphi(x)$. Equations (4) and (5) are applicable to all kinds of cantilevers and any external mass distribution. The eigenfrequencies, ω_n, the frequency shifts, $\Delta(\omega_n^2)$, and the cantilever width, $w(x)$, can be determined experimentally. The eigenmodes, u_n, of rectangular cantilevers can be obtained from the literature.[16] The modal shapes u_n of nonrectangular cantilevers can be determined by using the Ritz method.[14–16] The mass distribution $\varphi(x)$ along the cantilever is also often determined by the experimental conditions.

III. EXPERIMENTAL SECTION

To test the theoretical results a commercially available rectangular silicon cantilever (350 μm long, 0.03 N/m nominal spring constant, R-E, Mikromasch) and a V-shaped silicon nitride cantilever (196 μm long, 0.06 N/m nominal spring constant, V-D, Veeco) were exposed to relative humidity values in the range of $\sim$ 2% to $\sim$25% at 22 °C, similar to the experiments described in Ref. 17. Cantilevers were used as received. They can homogeneously adsorb small amounts of water at those humidity values. Experiments were performed with an AFM Explorer system (Thermo-Microscopes, Sunnyvale, CA, USA). Power spectral densities of thermal noise spectra were recorded with an external interface (National Instruments, USB-6251) as a function of humidity. Figures 1 and 2 display the experimentally obtained

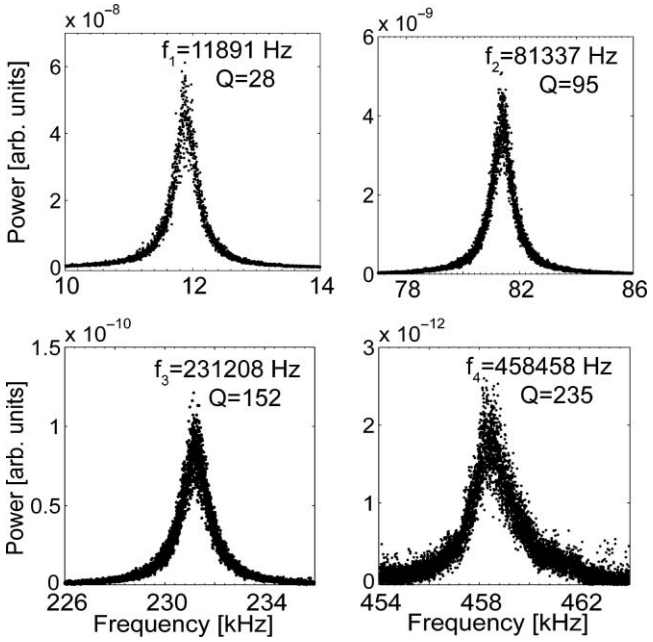

FIG. 1. Thermal noise power spectral densities of the first four flexural modes obtained with the rectangular cantilever. While the Q-factor increases with the mode number, the signal-to-noise ratio decreases.

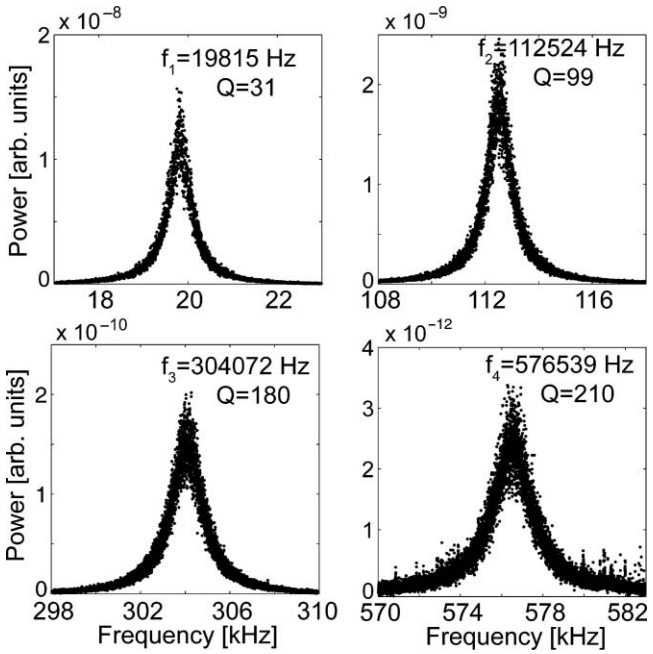

FIG. 2. Thermal noise power spectral densities of the first four flexural modes obtained with the V-shaped cantilever.

power spectral densities of the resonance peaks of the first four flexural modes for both the rectangular and V-shaped cantilevers together with their resonance frequency values at low humidity and the Q-factors. Resonant frequency values, Q-factors, and peak areas for each mode were determined during measurement with a homewritten LABVIEW™ routine from Lorentzian fits to the resonance peaks, similar to the procedure described in Ref. 18.

The resonant frequency values are based on the average of 50 individual spectra. The Q-factors showed fluctuations below 3% for all resonant peaks with no clear trend toward lower or higher values with increasing humidity. Q-factors can therefore be considered as constant and independent of humidity in our experiments.

The mass sensitivity or minimum detectable mass δM of the system is given by $\delta M = -(\delta(\omega_n^2)/\omega_n^2)M_{\mathrm{eff},n}^{\mathrm{cant}} \approx -2(M_{\mathrm{eff},n}^{\mathrm{cant}}/\omega_n)\delta\omega_n$,[19] where $\delta\omega_n$ is the minimum measurable frequency shift of mode n. Note that the mass sensitivity depends on the effective oscillating mass of the cantilever and hence the mass distribution of the accreted mass. In general, the mass sensitivity increases with increasing Q-factor. Thermal fluctuations, fluctuations in humidity as well as the signal-to-noise ratio, which decreases with increasing mode number in our experiment, all have an influence on the resulting sensitivity.[19] In order to determine the sensitivity in our experiments with thermally driven cantilevers we have taken the standard deviation, δf_n, of the measured resonant frequency values, f_n, at constant humidity as the minimum detectable frequency shift for each mode. The standard deviation values were determined from the fluctuations of 15 recordings of the resonant frequency values of the four modes at a fixed humidity. The values obtained were 4.3, 7.4, 7.5, and 8.7 Hz for modes 1–4 of the rectangular cantilever, respectively. The corresponding values for the V-shaped cantilever were 3.9, 7.6, 10.7, and 37.2 Hz. Error bars of the relative frequency shifts $\Delta(\omega_n^2)/\omega_n^2$ and hence sensitivities in our experiment are based on these standard deviations, δf_n, and are given by $\delta(\Delta(\omega_n^2)/\omega_n^2) \approx 2\sqrt{2}(\delta f_n/f_n)$.

IV. RESULTS AND DISCUSSION

If a single point mass is attached to a cantilever at position $x = L_{M_{\mathrm{ext}}}$, then $\varphi(x) = \delta(x - L_{M_{\mathrm{ext}}})$ and the relative frequency shift $\Delta(\omega_n^2)/\omega_n^2$ is proportional to $u_n^2(L_{M_{\mathrm{ext}}})$, which is the same as the result reported in Ref. 20. This finding can be easily extended to the case of several discretely attached masses[11] with Eq. (4).

If an area between $x = L_1$ and $x = L_2$ along a cantilever is modified such that a certain analyte can only adsorb in this region, then $\varphi(x) = 1$ for $L_1 \le x \le L_2$ and $\varphi(x) = 0$ elsewhere (see Fig. 3).

Equation (4) is particularly simple for rectangular cantilevers where w is constant. The total adsorbed mass can then be obtained from $\Delta M_{\mathrm{ext}} = -\Delta(\omega_n^2)/\omega_n^2 \Delta L / \int_{L_1}^{L_2} u_n^2(x)dx$, with $\Delta L = L_2 - L_1$. If the entire length of the plan view area can adsorb mass, i.e., $\Delta L = L$, then $M_{\mathrm{eff},n}^{\mathrm{cant}}$ corresponds to the total mass of the cantilever for all modes, and Eq. (1) can be used to determine the adsorbed mass simply based on the measured frequency shift and the total mass of the cantilever.

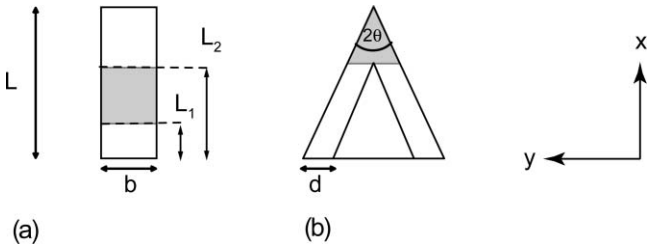

FIG. 3. Schematic top view of (a) rectangular and (b) V-shaped cantilevers. The shaded areas indicate external mass adsorption in these areas only, i.e., $\varphi(x) = 1$ for all x-coordinates corresponding to the shaded area and $\varphi(x) = 0$ elsewhere.

If ΔL does not correspond to the full length, then the $M_{\mathrm{eff},n}^{\mathrm{cant}}$ values will, in general, be different from the total cantilever mass and also different for different modes. Figure 4 summarizes the results for the relative frequency shifts, $\Delta(\omega_n^2)/\omega_n^2$, of the first four flexural modes of the rectangular and V-shaped cantilevers (see Fig. 3) that are widely available and for different adsorbed mass distributions. For V-shaped cantilevers the modal shapes u_n were obtained as described in Ref. 14. The resulting relative shifts were normalized to the $\Delta(\omega_1^2)/\omega_1^2$ value for full-length adsorption (encircled in Fig. 4). Note that the results for the rectangular and V-shaped cantilevers are independent from their specific dimensions if the entire cantilever can adsorb mass.

Figure 5 shows the experimentally obtained $\Delta(\omega_n^2)/\omega_n^2$ values for a relative humidity of up to ~25% and the first four flexural modes of both the rectangular and V-shaped cantilevers.

All modes show the same trend of $\Delta(\omega_n^2)/\omega_n^2$ over the humidity range studied for both the rectangular and V-shaped cantilevers, confirming the theoretical results for cantilevers that can adsorb mass over their full length. While the error bar is quite large for the first mode it is significantly smaller for the higher modes, indicating a relatively low mass sensitivity for the first mode and higher sensitivities for the higher modes. The minimum detectable mass values that are based

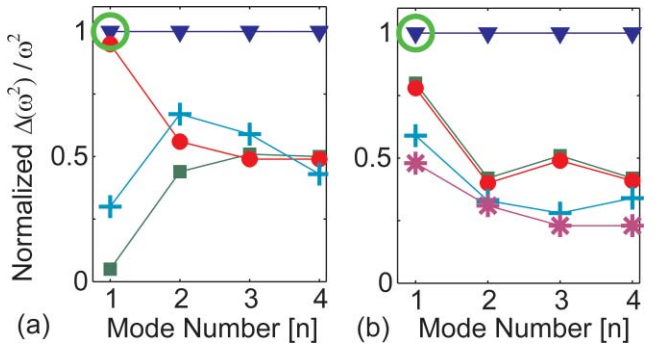

FIG. 4. (Color online) $\Delta(\omega_n^2)/\omega_n^2$ values for the first four flexural modes of (a) rectangular and (b) V-shaped cantilevers and several mass distributions $\varphi(x)$. $\Delta(\omega_n^2)/\omega_n^2$ in each figure is normalized to the encircled $\Delta(\omega_1^2)/\omega_1^2$ value. Mass distributions on rectangular cantilevers are for $L_1 = 0$, $L_2 = L$ (▼), $L_1 = 0$, $L_2 = L/2$ (■), $L_1 = L/2$, $L_2 = L$ (●), and $L_1 = L/4$, $L_2 = 3L/4$ (+). Mass distributions on the V-shaped cantilevers ($2\theta = 51.2°$) are for adsorption over the full length (▼) and for adsorption on the triangular part only (see Fig. 3): V-A (■) $L = 115$, $d = 25$; V-B (●) $L = 196$, $d = 41$; V-C (+) $L = 115$, $d = 17$; V-D (*) $L = 196$, $d = 23$ (all dimensions are in micrometers).

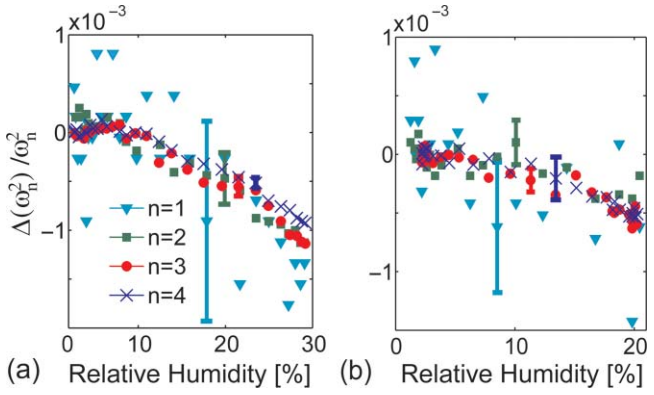

FIG. 5. (Color online) Experimentally determined $\Delta(\omega_n^2)/\omega_n^2$ values for (a) a rectangular cantilever and (b) a V-shaped cantilever and the first four flexural modes at different relative humidity values. The cantilevers can adsorb water over their full length. Error bars are based on the experimentally determined fluctuations in the resonant frequency values (standard deviation) at constant humidity. Only one error bar for each mode is shown for clarity.

on the fluctuations in the resonant frequencies at constant humidity can be converted to water film thickness, which is the parameter of interest here. The resulting sensitivities in the film thickness are 13.7, 3.2, 1.1, and 0.7 Å based on the first four modes of the rectangular cantilever, respectively. The corresponding values for the V-shaped cantilever are 8.6, 3.0, 1.5, and 2.8 Å. The decrease in the sensitivity of the fourth mode in case of the V-shaped cantilever is due to the relatively large fluctuations in that resonant frequency of the cantilever used. The sensitivity values obtained underline that the accreted mass and the thickness of the film adsorbed onto a cantilever surface can be determined with high accuracy when using higher flexural modes. The reason is that the absolute frequency shifts $\Delta(\omega_n^2)$ are higher for the higher modes granting them a higher accuracy for low masses in general. The water film thickness itself can be obtained with Eq. (4) and amounts to around 7 Å at ~25% relative humidity. This result is in good agreement with values reported in the literature.[21]

Note that stress induced by the adsorbed mass would be reflected by different $\Delta(\omega_n^2)/\omega_n^2$ values for different modes at constant humidity. The simultaneous measurement of $\Delta(\omega_n^2)/\omega_n^2$ values for several flexural modes in combination with Eq. (4) could therefore be exploited to separate frequency changes that are due to mass from those that are due to stress.

V. CONCLUSIONS

In summary, we derived expressions that allow for the determination of the total attached mass on cantilever sensors under any mass distribution and for all flexural modes. We demonstrated the applicability of the equations for the first four flexural modes in the case mass can adsorb over the full length of a cantilever and for two different types of cantilevers. Small amounts of mass can be determined accurately and precisely for thermally driven cantilevers, in particular when using higher flexural modes, since they show a higher sensitivity toward an accreted mass than the first flexural mode. The simultaneous measurement of $\Delta(\omega_n^2)/\omega_n^2$ for several modes opens up interesting perspectives to determine both the adsorbed mass and the stress caused by it and therefore might also allow it to gain information about the interactions inside thin films and between thin films and substrates.

ACKNOWLEDGMENTS

Financial support from the University of St. Andrews is gratefully acknowledged.

[1] P. S. Waggoner and H. G. Craighead, Lab Chip **7**(10), 1238 (2007).
[2] N. McLoughlin, S. L. Lee, and G. Hähner, Lab Chip **7**(8), 1057 (2007).
[3] N. McLoughlin, S. L. Lee, and G. Hähner, Appl. Phys. Lett. **89**(18), 184106 (2006).
[4] M. Spletzer, A. Raman, and R. Reifenberger, Appl. Phys. Lett. **91**(18), 184103 (2007).
[5] Y. T. Yang, C. Callegari, X. L. Feng, K. L. Ekinci, and M. L. Roukes, Nano Lett. **6**(4), 583 (2006).
[6] M. Li, H. X. Tang, and M. L. Roukes, Nat. Nanotechnol. **2**(2), 114 (2007).
[7] B. Ilic, S. Krylov, M. Kondratovich, and H. G. Craighead, Nano Lett. **7**(8), 2171 (2007).
[8] D. Ramos, M. Calleja, J. Mertens, A. Zaballos, and J. Tamayo, Sensors **7**(9), 1834 (2007).
[9] A. K. Naik, M. S. Hanay, W. K. Hiebert, X. L. Feng, and M. L. Roukes, Nat. Nanotechnol. **4**(7), 445 (2009).
[10] S. Dohn, R. Sandberg, W. Svendsen, and A. Boisen, Appl. Phys. Lett. **86**(23), 233501 (2005).
[11] S. Dohn, S. Schmid, F. Amiot, and A. Boisen, Appl. Phys. Lett. **97**(4), 044103 (2010).
[12] E. A. Wachter and T. Thundat, Rev. Sci. Instrum. **66**(6), 3662 (1995).
[13] I. U. Vakarelski, S. A. Edwards, R. R. Dagastine, D. Y. C. Chan, G. W. Stevens, and F. Grieser, Rev. Sci. Instrum. **78**(11), 116102 (2007).
[14] G. Hähner, Ultramicroscopy **110**(7), 801 (2010).
[15] R. Courant and D. Hilbert, *Methoden der Mathematischen Physik I* (Springer Verlag, Heidelberg, 1968).
[16] S. Timoshenko, D. H. Young, and W. Weaver, Jr., *Vibration Problems in Engineering*, 4th ed. (Wiley, New York, 1974).
[17] G. Y. Chen, T. Thundat, E. A. Wachter, and R. J. Warmack, J. Appl. Phys. **77**(8), 3618 (1995).
[18] J. L. Hutter and J. Bechhoefer, Rev. Sci. Instrum. **64**(7), 1868 (1993).
[19] K. L. Ekinci, Y. T. Yang, and M. L. Roukes, J. Appl. Phys. **95**(5), 2682 (2004).
[20] S. Dohn, W. Svendsen, A. Boisen, and O. Hansen, Rev. Sci. Instrum. **78**(10), 103303 (2007).
[21] D. B. Asay and S. H. Kim, J. Phys. Chem. B **109**(35), 16760 (2005).